ICSO 2016

International Conference on Space Optics

Biarritz, France

18–21 October 2016

Edited by Bruno Cugny, Nikos Karafolas and Zoran Sodnik

Co2 remote detection using a 2-um dial instrument

Erwan Cadiou

Dominique Mammez

Jean-Baptiste Dherbecourt

Guillaume Gorju

et al.

esa icso proceedings cnes

International Conference on Space Optics — ICSO 2016, edited by Bruno Cugny, Nikos Karafolas, Zoran Sodnik, Proc. of SPIE Vol. 10562, 105621V · © 2016 ESA and CNES
CCC code: 0277-786X/17/$18 · doi: 10.1117/12.2296148

CO_2 REMOTE DETECTION USING A 2-µM DIAL INSTRUMENT

Erwan Cadiou[1, 2], Dominique Mammez[2], Jean-Baptiste Dherbecourt[1], Guillaume Gorju[1], Myriam Raybaut[1], Jean-Michel Melkonian[1], Antoine Godard[1], Jacques Pelon[3], Michel Lefebvre[1]
[1] *ONERA, The French Aerospace Lab, Chemin de la Hunière, F-91761 Palaiseau cedex, France*
[2] *CNES, centre de Toulouse, 18 avenue Edouard Belin, F-31401 Toulouse cedex 9, France*
[3] *LATMOS, Université Pierre et Marie Curie, 4 Place Jussieu Paris, France*

I. INTRODUCTION

Several possible future spatial lidar missions (MERLIN EXCALIBUR ASCENDS) are intended to measure major greenhouse gases (CO_2, H_2O, CH_4) in order to better understand their cycle and their impact on climate change. One of the challenges of these missions is to get robust sources emitting at least two wavelengths (inside and outside an absorption line of the gas) to perform the differential absorption lidar (DIAL) measurement [1,2].

In this paper, we present long range atmospheric concentration measurements with an instrument able to monitor the three interesting gases. The lidar transmitter is based on a nested cavity optical parametric oscillator (NesCOPO) [3]. Such OPO configuration enables us to demonstrate a wide tunability in the 1.98 – 2.3 µm range, without an additional injection seeding device to seed the OPO, thus allowing us to target several species. Such generic architecture can be interesting for a space-borne instrument since it allows i) a single instrument development and spatialization process for different missions, ii) possible in-flight instrument reconfiguration to target a different species than originally specified, iii) a possible single mission for different green-house gases measurement.

II. 2 µm TRANSMITTER BENCH

Our experimental set-up is depicted in Fig. 1. The pump laser is a high energy (100 mJ) single frequency Nd:YAG laser, delivering 12 ns pulses at a 30 Hz repetition rate. The Master Oscillator Power Amplifier (MOPA) parametric frequency converter allows to reach a high pulse energy in the mid-infrared while maintaining high spectral and spatial quality. The oscillator is based on a nested cavities doubly resonant optical parametric oscillator (NesCOPO) with a 10 mm long type II periodically poled lithium niobate (PPLN) nonlinear crystal used close to degeneracy, composed of several gratings with different poling periods.
Single-longitudinal-emission operation of the device is obtained with an appropriate dissociation of the two cavity lengths in the 10 % range, leading to only one single coincidence of signal and idler modes within the parametric gain bandwidth (PGB) (Fig. 2(b)).
Relative shifting of the signal and idler frequency combs allows Vernier frequency sampling of the emitted single-frequency radiation [3,4].
The NesCOPO radiation is then amplified to the >10 mJ energy level, which is achieved by pre-amplification of the NesCOPO output using a 25 mm long type 0 PPLN crystal, followed by bulk KTP amplifiers. To maintain a high beam quality at the output, the four bulk 20 mm long KTP amplifiers are oriented in a walk-off compensation configuration, and a filtering mirror, highly reflective for the idler wave, is inserted between crystal 2 and crystal 3 in order to mitigate back-conversion defects. Indeed, it has already been shown that such idler suppression scheme reduces saturation and thus limits its detrimental effects such as beam quality deterioration [5].

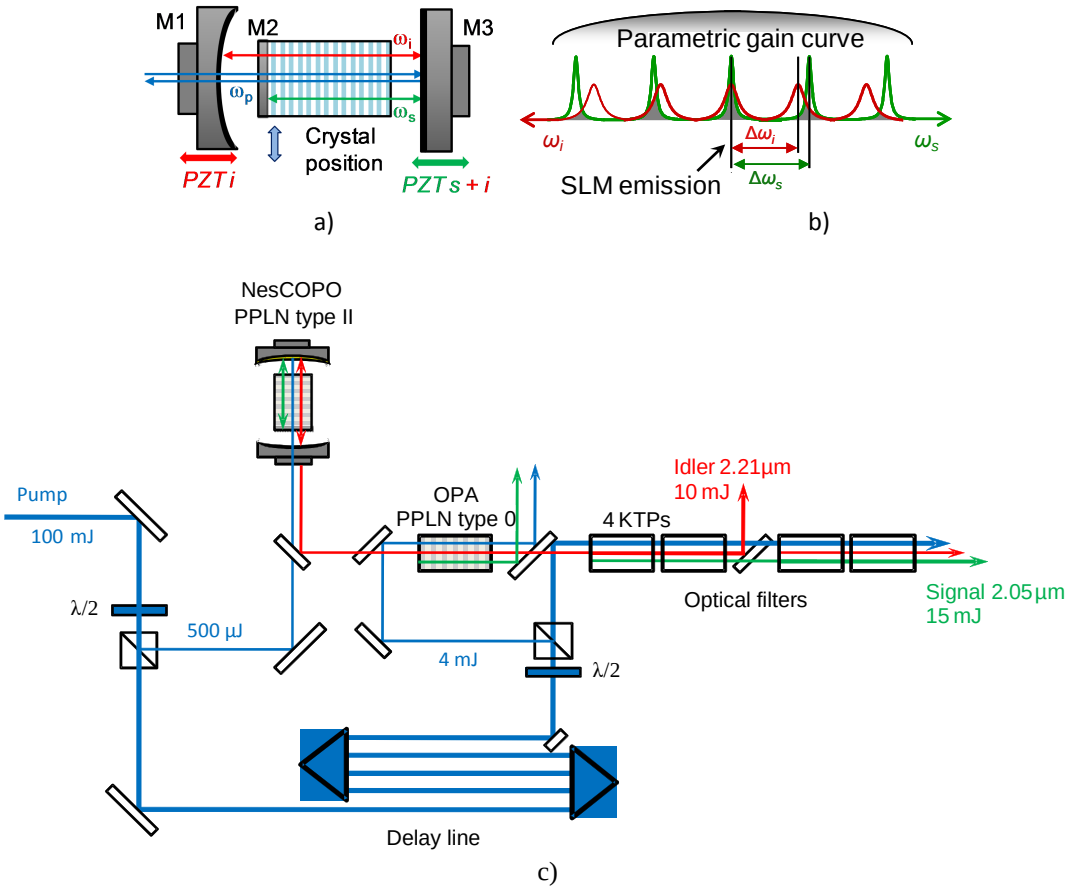

Fig. 1. NesCOPO device a), Signal and Idler mode coincidences: with adequate dissociation, a single frequency is emitted without injection seeding b), Schematic diagram of the MOPA overall design c).

The performances of the source are measured at 2.05 µm, in the vicinity of the R30 CO_2 line. We demonstrate a typical 50 % pump depletion after the KTP amplification stages, and the extracted signal energy at 2.05 µm is higher than 15 mJ for 60 mJ of incident pump on the KTP amplifier stage. The signal beam propagation factor was measured from the 16% - 84% knife-edge widths method, and estimated to be $M^2 < 1.1$ for both vertical and horizontal directions.

The signal frequency stability is measured shot by shot, after second harmonic generation, using a WSU 10 High Finesse wavemeter operating in the visible – near IR range (Figure 2). The signal frequency stability is better than 3 MHz rms, over a few tens of seconds. It is thus twice better than the pump frequency variations, which result from the Nd:YAG cavity mirror dithering. Indeed, the 3 MHz signal frequency fluctuations are attributed to the residual electronic noise of the PZT driver measured to be of around 2 MHz rms. This could be further improved using better opto-mechanical design and lower-noise piezoelectric transducers. Such work is currently under investigation in several on-going projects. The signal cavity mirrors are highly reflective while the idler cavity consists of a highly reflective mirror and an output coupler (of 80 % reflectivity to the idler wave).

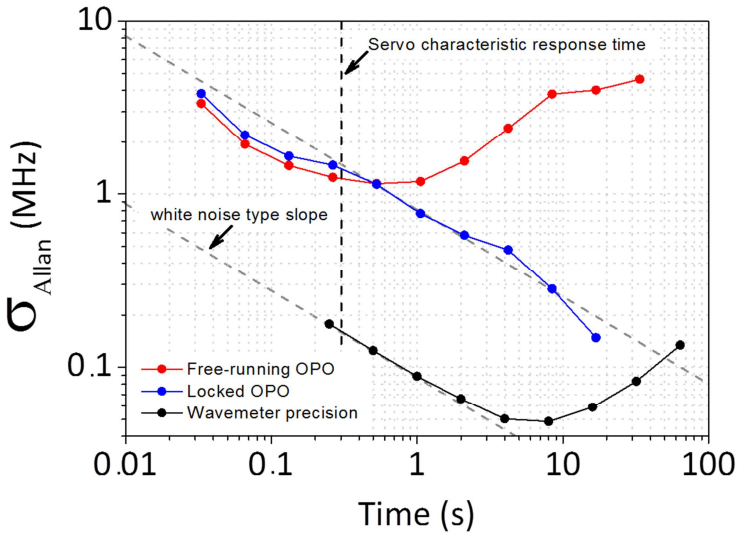

Fig. 2. Allan deviation of the signal frequency emitted by our MOPA set-up, in free-running (open loop curve), with active control (closed loop curve) of mirror M1 position. The wavemeter is injected with a high frequency stability Rb atomic transition locked source for calibration and its frequency stability is measured (Wavemeter).

III. CAPABILITY OF THE BENCH FOR CO_2, H_2O AND CH_4 REMOTE SENSING

To validate experimentally the multi-species capability of our optical source, we performed absorption measurements in gas cells filled with the different species, namely CO_2, CH_4 and H_2O.
These three species were addressed using two different quasi-phase matching grating periods. For CO_2 and H_2O, the signal is used. For CH_4 the idler is used. The absorptions lines addressed with our source with the operating temperature of the NesCOPO crystal are presented on the table 1.

Table 1. NesCOPO crystal operating temperatures to target the different species

Species	OPO temperature (°C)	Wavelength (nm)
CO_2	88.5 °C	λ_s = 2050.97 nm
CH_4	90 °C	λ_i = 2211.25 nm
H_2O	94.5 °C	λ_s = 2056.64 nm

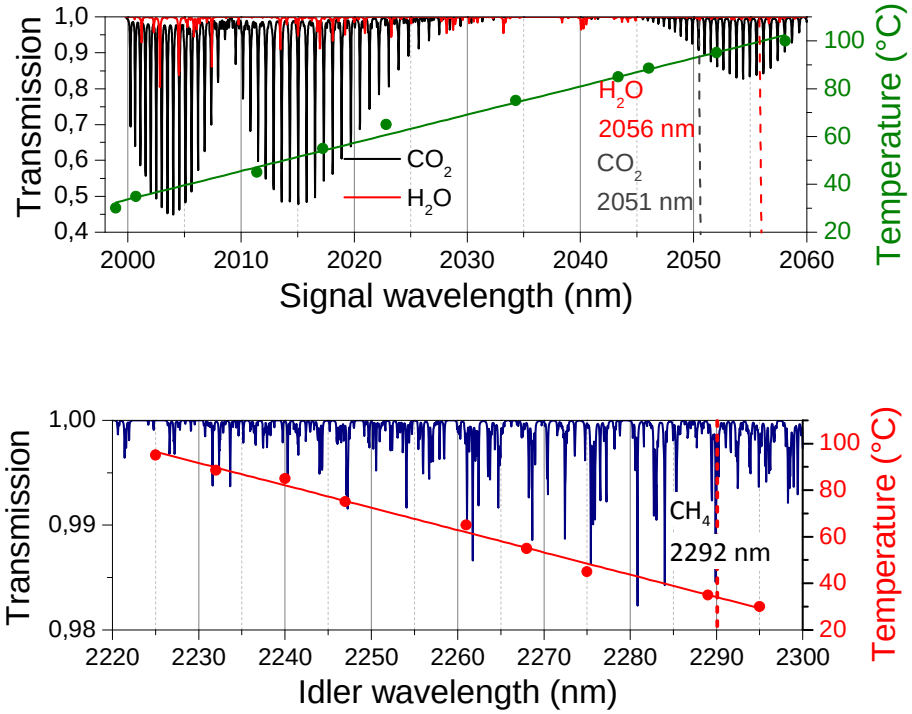

Fig. 3. Wavelength range reachable by temperature tuning of the amplified NesCOPO over two adjacent quasi-phase matching (QPM) periods: (a) signal wavelength with the 14.369 µm QPM period, used for H_2O and CO_2 measurements; (b) idler wavelength with the 14.38 µm QPM period, used for CH_4, and corresponding green-house gases spectral lines (dots: experimental data, lines: HITRAN simulation of atmospheric CO_2 (black line), CH_4 (blue line) and H_2O (red line) concentrations over a 100 m path, vertical dashed lines: absorption lines for spatial applications).

To realize the absorption measurement, we use an equivalent experimental setup for the three species. A small amount of the signal energy (several µJ) delivered by the optical source is injected in a single mode fiber (SMF 28 fiber) coupled to a 50/50 coupler specified at 1.5 µm. In practical at 2 µm its performances are closer to a 25/75 coupler. One of the coupler output is coupled to the gas cell, coupled a long wavelength InGaAs detector. This is our transmission measurement line. The second output coupler, called reference, is directly connected to an identical long wavelength InGaAs detector, thus creating a reference signal to correct the transmission measurement from the source intensity fluctuations.

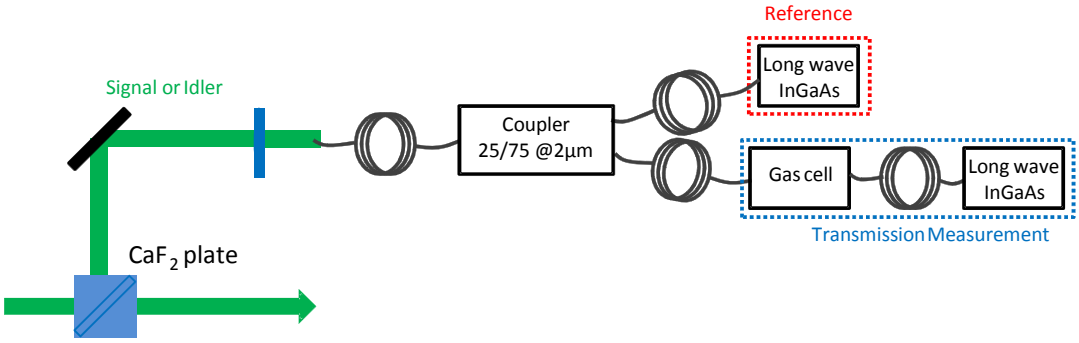

Fig. 4. Transmission measurement of a gas cell: experimental set-up.

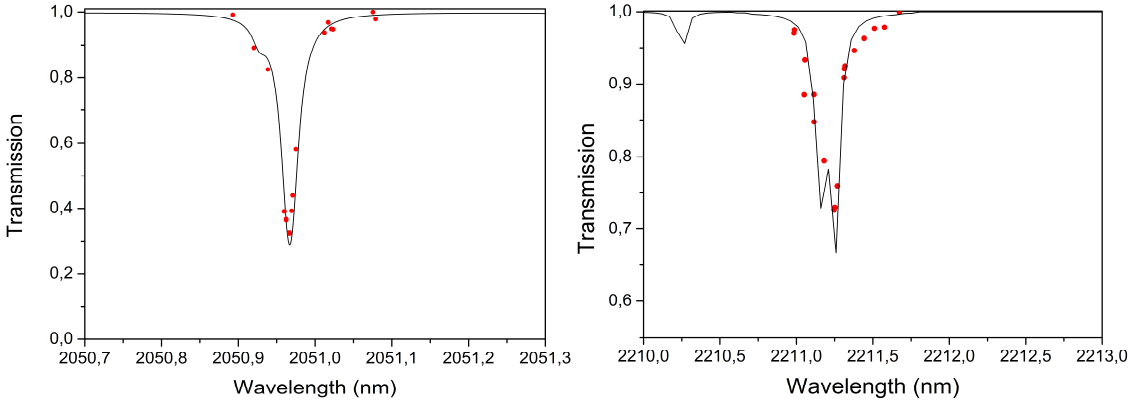

Fig. 5. Obtained gas cell transmissions : CO_2 a), and CH_4 b).

Three different gas cells were used. On the one hand, we use 80 cm long commercial pigtailed multi-pass cells bought in 2010 for carbon dioxide or water. These two cells were specified to contain 100% of the species at 200 Torr. On the other hand, we use a 10 cm long massive cell filled with 100% of methane at atmospheric pressure and temperature.
We adjust the position of the two PZT actuators to tune the wavelength of the source over the absorption lines. At set crystal position and set temperature, the signal wavelength can be adjusted over 1 nm, corresponding to the parametric gain bandwidth of our non-linear crystal. The average energy of the transmission and reference are averaged over 16 shots using an oscilloscope. The theoretical transmission of the cells is calculated from the spectroscopic Hitran database. The results of these transmission measurements are presented only for CO_2 and CH_4 on the Figures 5(a) and 5(b) respectively. Water measurement was prevented by the low depth of the water absorption line that was addressed here (only 3%), close to our signal to noise measurement ratio. For the two other species the measured transmission and the simulation are in quite good agreement.

IV. FIRST DIAL EXPERIMENTS ON ATMOSPHERIC CO_2

The emitter output is coupled with a receiver collecting the backscattered light.
It consists of a Newton telescope which focuses the backscattered laser radiation on a commercial InGaAs amplified photodiode. To increase the field of view of the telescope a short focal lens is placed in front of the detector. The resulting field of view of 800 µrad is adapted to the transmitted laser beam. Emission and reception axes overlap and are oriented at 45° from the vertical, which enables to reach clouds at the top of the boundary layer (about 600 m).

Both lidar and normalization signals are acquired with a 500 MHz digitizer, and averaged over 10,000 shots corresponding to 5 minutes acquisition time. The measurements are performed with ON and OFF wavelength switched on a shot-to-shot basis. First experimental measurements have been obtained by targeting the R30 absorption line of CO_2 at 2051 nm. Typical backscattered signal are shown in Fig. 6 a). Given the sensitivity of our commercial photodiode, backscattered signals could be acquired within several hundreds of meters. Given the 45° elevation angle of our line of sight, echoes due to clouds could also be observed. In Fig. 6 b), we can see some shot by shot backscattered signals due to the clouds echoes. The intensity modulation is due to the CO_2 ON/OFF line probing, resulting in an attenuation of the ON signals due to atmospheric CO_2 absorption. Thus, the optical depth measured on clouds matches with a 397 ppm CO_2 mixing ratio with a ± 3 ppm uncertainty (Fig. 6 c)). This result has been obtained by performing an Integrated Path measurement over 1200 m (distance between the LIDAR output and the cloud). The uncertainty of +/- 3 ppm corresponds to the variation of the slope coefficient measured on figure 6(c) between 200m and 1200 m.

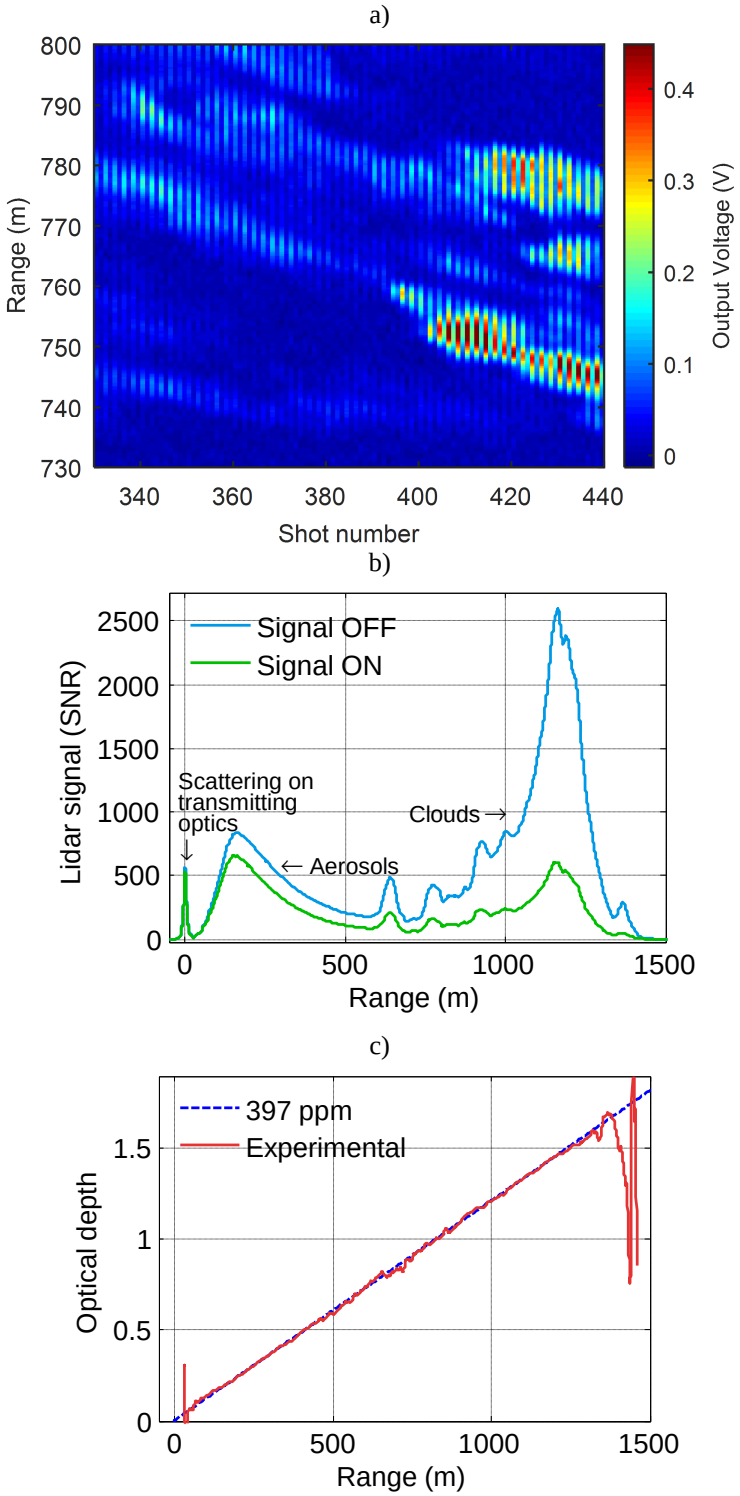

Fig. 6. (a) OFF-line and ON-line return signals. Averaging over 10,000 shots and a 15 MHz numerical filtering have been applied to both signals. (b) Zoom on some ON/OFF shot by shot backscattered signals: the shot-to-shot modulation of the backscattered signal is due to the CO_2 absorption (c) Differential optical depths versus range for experimental data and for a theoretical homogeneous mixing ratio of 397 ppm.

V. CONCUSION

We presented the first DIAL measurement using a NesCOPO based emitter, allowing to target the three main green-house gases of interest. Preliminary DIAL experiments were presented on CO_2. Future work will be dedicated to i) the instrument sensitivity improvement, range improvement, through optimization of the receiver

and transmitter units, ii) the overall instrument TRL improvement through miniaturization of the emitter unit, use of specifically developed non-linear crystals for increased energy efficiency and ruggedness, and iii) measurements on other species, namely CH_4 and H_2O.

REFERENCES

[1] G. Ehret, C. Kiemle, M. Wirth, A. Amediek, A. Fix, and S. Houweling, Appl. Phys. B **90**, pp. 593, 2008.
[2] J. Caron and Y. Durand, Appl. Opt. **48**, pp. 5413, 2009.
[3] B. Hardy, A. Berrou, S. Guilbaud, M. Raybaut, A. Godard, and M. Lefebvre, Opt. Lett. 36(5), 678-680, 2011.
[4] J. Barrientos Barria, D. Mammez, E. Cadiou, J.-B. Dherbecourt, M. Raybaut, T. Schmid, A. Bresson, J.-M. Melkonian, A. Godard, J. Pelon, and M. Lefebvre, "Multispecies high-energy emitter for CO2, CH4, and H2O monitoring in the 2 µm range," Opt. Lett., 39, pp. 6719–6722, 2014.
[5] G. Arisholm, R. Nordseth, and G. Rustad, Opt. Express **12**, pp. 4189, 2004.